# Zernike moments descript of solar and astronomical features: Python code

Hossein Safari[1,2]*, Nasibe Alipour[3]†, Hamed Ghaderi[1] and Pardis Garavand[1]

[1]Department of Physics, Faculty of Science, University of Zanjan, University Blvd., 45371-38791, Zanjan, Iran
[2]Observatory, Faculty of Science, University of Zanjan, University Blvd., 45371-38791, Zanjan, Iran
[3] Department of Physics, University of Guilan, Rasht, 41335-1914, Iran;

## 1 Abstract

Due to the massive increase in astronomical images (such as James Web and Solar Dynamic Observatory), automatic image description is essential for solar and astronomical. Zernike moments (ZMs) are unique due to the orthogonality and completeness of Zernike polynomials (ZPs); hence valuable to convert a two-dimensional image to one-dimensional series of complex numbers. The magnitude of ZMs is rotation invariant, and by applying image normalization, scale and translation invariants can be made, which are helpful properties for describing solar and astronomical images. In this package, we describe the characteristics of ZMs via several examples of solar (large and small scale) features and astronomical images. ZMs can describe the structure and morphology of objects in an image to apply machine learning to identify and track the features in several disciplines.

*E-mail: safari@znu.ac.ir
†E-mail: nasibealipour@gmail.com

# 2 Introduction

Objects recognition in images has been developed in several disciplines (e.g., Goshtasby, 1985; Heywood and Noakes, 1995; Aschwanden, 2010; Zheng et al., 2015; Moradkhani et al., 2015; Noori et al., 2019). Recently, feature extraction for machine learning of object finding and tracking based on image moments was investigated (Honarbakhsh and Morra, 2023). Moments are a class of image description (e.g., Gonzaga and Ferreira Costa, 1996; Teh and Chin, 1988).
Since the image data of various fields such as biology, medicine, optics, astronomy, and solar physics are vastly recorded, these images' descriptions are out of manual analysis. The image moments are quantities that describe an image's shape, objects, and structure.
Zernike moments (ZMs) map an image to a complex number series (Gonzalez and Faisal, 2019; Hu, 1962; Flusser, 2000; Nayak et al., 2018; Zhang et al., 2015; Doerr and Florence, 2020). ZMs are a family of orthogonal moments due to the property of Zernike polynomial functions (Mukundan et al., 2001). Due to the exponential phase term of complex Zernike polynomials, the magnitude of ZMs is rotation invariant. In the lecture, a comprehensive review of Zernike polynomials and applications where explain (Mukundan and Ramakrishnan, 1995; Belkasim et al., 1996; Zhenjiang, 2000; Gu et al., 2002; Chong et al., 2003; Sim et al., 2004; Mitzias and Mertzios, 2004; Papakostas et al., 2006, 2007; Sadeghi et al., 2021; Niu and Tian, 2022; Capalbo et al., 2022).
Recently, ZMs have been widely used for describing the characteristics of various digital images in different disciplines (Gu et al., 2002; Chong et al., 2003; Sim et al., 2004; Mitzias and Mertzios, 2004; Papakostas et al., 2006, 2007; Sadeghi et al., 2021; Niu and Tian, 2022; Capalbo et al., 2022).
The ZMs, as a basis of machine learning, were applied for the identification of solar small-scale brightenings (Yousefzadeh et al., 2016; Javaherian et al., 2014; Shokri et al., 2022; Hosseini Rad et al., 2021) and small-scale (mini) dimmings (Alipour et al., 2012; Honarbakhsh et al., 2016; Alipour et al., 2022). The ZMs are valuable features for classifying solar flaring and non-flaring active regions (Raboonik et al., 2016; Wheatland et al., 2017; Alipour et al., 2019) that developed a tool of solar flare for casting.
The layout this paper is: Sections 3 and 4 describe the Zernike polynomials and Zernike moments, respectively. Section 5 provides an overview of Python code. Section 6 gives the conclusions.

# 3 Zernike polynomials

The ZPs are a complete set of orthogonal continuous functions in a unit disk. The even ZPs with order $n$ and repetition $m$ in the polar coordinate are given by

$$ZP_{pq}(r,\theta) = R_{pq}(r)\ \cos(q\,\theta) \tag{1}$$

and the odd ZPs function is defined by

$$ZP_{p-q}(r,\theta) = R_{pq}(r)\ \sin(q\,\theta) \tag{2}$$

where the radial distance in a unit circle is $0 \leq r \leq 1$ and the azimuths angle is $0 \leq \theta \leq 2\pi$.
The radial polynomials for a given set of $p$ and $q$ are defined by

$$Rpq(r) = \sum_{k=0}^{\frac{p-q}{2}} \frac{(-1)^k\,(p-k)!}{k!\,\left(\frac{p+q}{2}-k\right)!\,\left(\frac{p-q}{2}-k\right)!} r^{p-2k} \tag{3}$$

in which $p - q$ = even and $|q| \leq p$. The ZPs satisfy the following orthogonality property as,

$$\int_0^{2\pi}\int_0^1 V_{pq}^* V_{p'q'} r\,dr\,d\theta = \frac{\pi}{p+1}\delta_{pp'}\delta_{qq'}, \tag{4}$$

where $\delta$ indicates the Kronecker delta function.
Figure 1 represents the radial function $R_{pq}$ for a set of $p$ and $q$ in versus radial distance of polar coordinate. We observe that the radial functions increase oscillations by increasing the order number $p$. This property of ZPs' radial functions is one of the main reasons for applying the ZMs to describe an image in a polar coordinate.
Figure 2 displays $Z_{pq}$ for a set of order number $p = 0,\ 1,\ 2$, and 3 in polar coordinates. The figure shows that each Zernike polynomials have unique radial and azimuthal structures in polar coordinates. This essential characteristic of Zernike polynomials is the main reason for describing an image based on the set of complex Zernike polynomials (combination of even and odd Zernike functions in complex number plane), which maps to a unit circle.

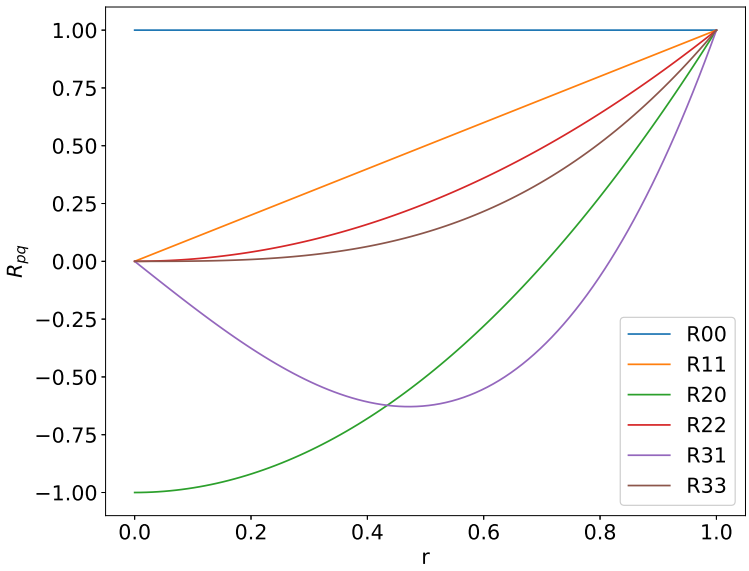


Figure 1: The radial function $R_{pq}$ for a set of $p$ and $q$ in versus radial distance of polar coordinates.

# 4 Zernike Moments

The reason to describe an image by a set of functions is due to The uniqueness theorem. This theorem explains that the moments are uniquely discriminated for a given image (Gonzaga and Ferreira Costa, 1996). Contrariwise, we can reconstruct the original image using the set of moments. Moments can specify the properties, such as the centroid of an image, its orientation, and the geometry of the objects. Raw and central moments were defined by Gonzaga and Ferreira Costa (1996); Grubbström and Tang (2006).

The Zernike moments (ZMs) express an image in a set of complex numbers using the Zernike polynomials $V_{pq} = ZP_{pq} * (\text{even}) + iZP_{pq}(\text{odd})$ (Mukundan et al., 2001). The image coordinates $(x, y)$ must be transformed into the polar coordinate. The circle's center in polar coordinates is the centroid of an image. For an image function $I(r, \theta)$, the ZM is given by,

$$Z_{pq} = \frac{p+1}{\pi} \int_0^{2\pi} \int_0^1 I(r,\theta) V_{pq}^* r dr d\theta. \tag{5}$$

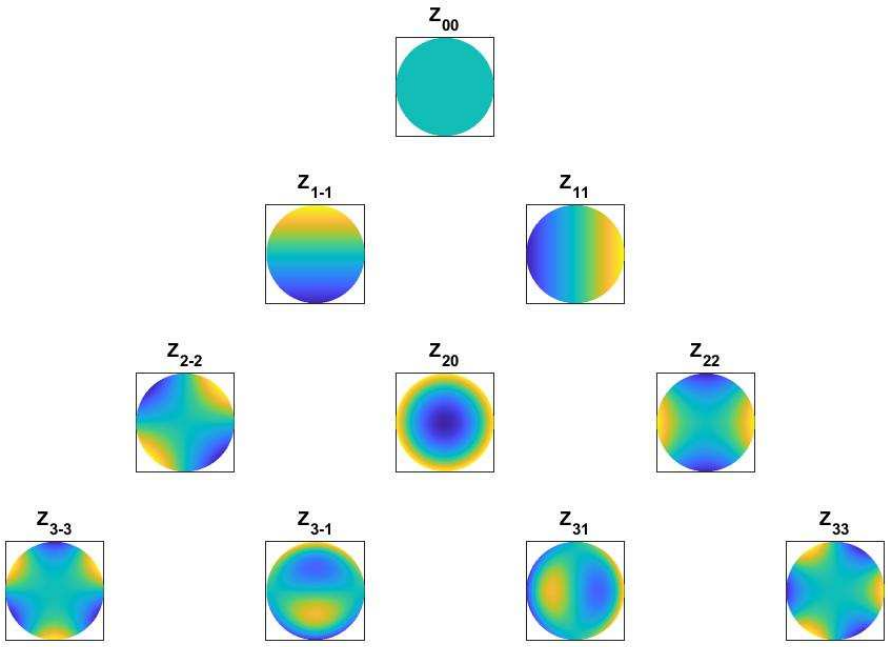


Figure 2: The Zernike polynomial $Z_{pq}$ for a set of order number $p = 0$ (first row), $p$ =1 (second row), $p$ =2 (third row), and $p$ =3 (fourth row).

For a digital image with M × N pixels, the ZMs are introduced by

$$Z_{pq} = \frac{p+1}{\pi} \sum_{i=0}^{M-1} \sum_{j=0}^{N-1} I(i,j) R_{pq}(r_{ij}) \exp(-ip\theta_{ij}), \tag{6}$$

where $r_{ij} = \sqrt{x_i^2 + y_j^2}$ and $\theta_{ij} = \arctan(\frac{y_j}{x_i})$ are the image cell mapped to a unit disk (Wolf et al., 2011).
The Zernike moment array includes elements for a set of order $p$=0 to a maximum order number $P_{\max}$. So, the length of Zernike moments ($NZMs$) is introduced by (Alipour et al., 2019)

$$NZMs = \sum_{p=0}^{P_{\max}} (p+1). \tag{7}$$

The reconstructed image ($I_R$) is given by an inverse transformation Khotanzad and Hong (1990) as follow,

$$I_R(r,\theta) = \sum_{p=0}^{P_{\max}} \sum_{q} Z_{pq} V_{pq}(r,\theta). \tag{8}$$

Using the original and reconstructed images, we obtain the reconstruction error as

$$\mathrm{e}^2(\mathrm{I}, \mathrm{I_R}) = \frac{\sum_{\mathrm{i}=0}^{\mathrm{M}-1} \sum_{\mathrm{j}=0}^{\mathrm{N}-1} (\mathrm{I(i,j)} - \mathrm{I_R(i,j)})^2}{\sum_{\mathrm{i}=0}^{\mathrm{M}-1} \sum_{\mathrm{j}=0}^{\mathrm{N}-1} (\mathrm{I(i,j)})^2}. \tag{9}$$

Figure 3 shows a full disk AIA image at 171 Å inset a solar coronal bright point and the Zernike moments' maximum order 25. The Zernike moments include the imaginary and real parts (panel b). The structure of the moment series is represented by the absolute normalized Zernike moments versus labels.
Figure 4 represents an original (face) image and reconstructed images with different maximum order numbers. We observe that the reconstructed image at $P_{\max}$= 10 deviated from the original image, but the reconstructed image at 45 well matched the original image. Also, increasing the maximum order number of the reconstructed image showed noisy image may be due to the discrete behavior of a digital image.

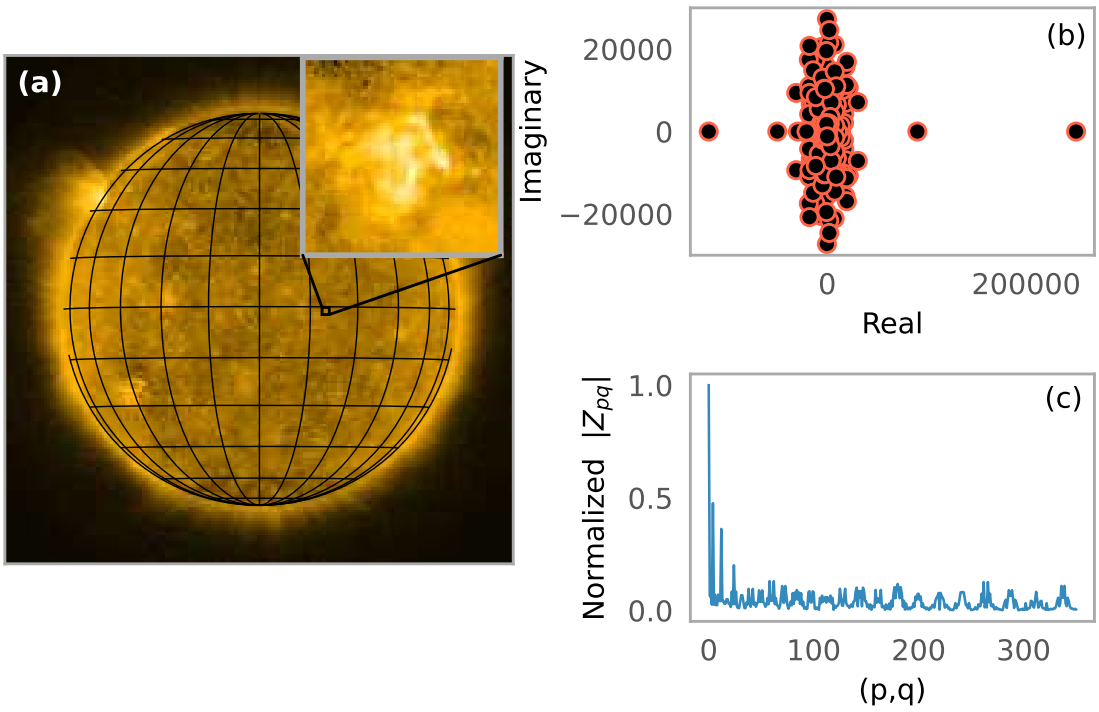


Figure 3: The full disk AIA image at 171 Å that inset a solar coronal bright point (a), the imaginary and real parts of Zernike moments for a maximum order number of 25 (b), and the absolute normalized Zernike moments versus labels $(p, q)$ (c).

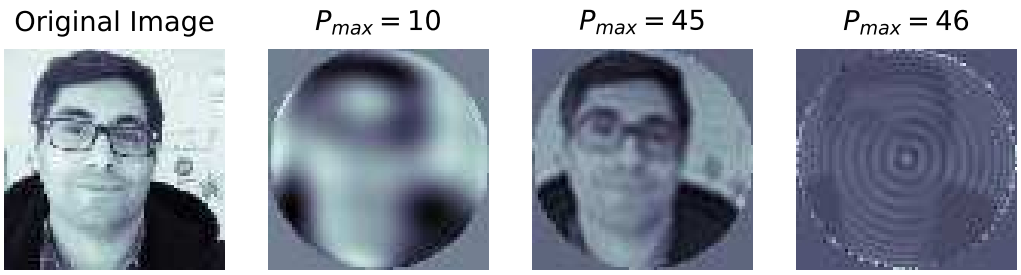


Figure 4: From left to right panels represent the original (face: Hossein Safari) image and reconstructed images with the different maximum order numbers ($P_{\max}$= 10, 45, and 46), respectively.

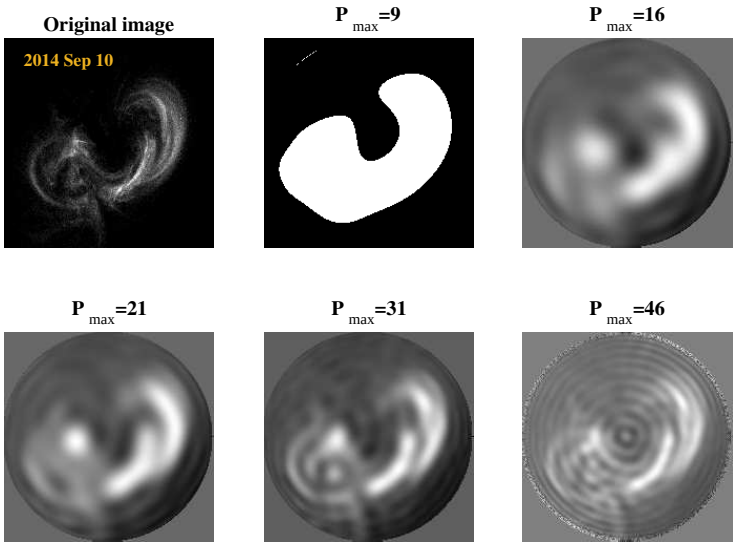


Figure 5: An active region (sigmiod: left top panel) from SDO/AIA at 94 Å. The reconstructed images for $P_{\max}$= 9, 16, 21, 31, and 46 (Alipour et al., 2019).

Figure 5 displays a solar active region (AR) in Solar Dynamics Observatory/Atmospheric Imaging Assembly (SDO/AIA) at 94 Å. An sigmiod event and the reconstructed images with various maximum order numbers ($P_{\max}$) are shown. For small $P_{\max}(< 10)$, the overall shape of the sigmiod was reconstructed. We observe that with increasing the $P_{\max}$, the reconstructed image approaches the original image at $P_{\max}$ (= 31). We also see that the reconstructed image deviates from the original for large $P_{\max}$ (= 46).
Figure 6 shows the original and reconstructed images with the different maximum order numbers for a spiral galaxy (top row), elliptical galaxy (middle row), and irregular galaxy (bottom row). We find the minimum reconstruction error for $P_{\max}$= 45 for spiral, elliptical, and irregular galaxies. For more or less value than 45, the reconstructed image deviated from the original image. In the case of minimal reconstruction error, we expect to well match objects, shapes, and their orientations or morphologies in reconstructed images and original images.
ZPs include orthogonal functions; hence moments give the properties of an image.

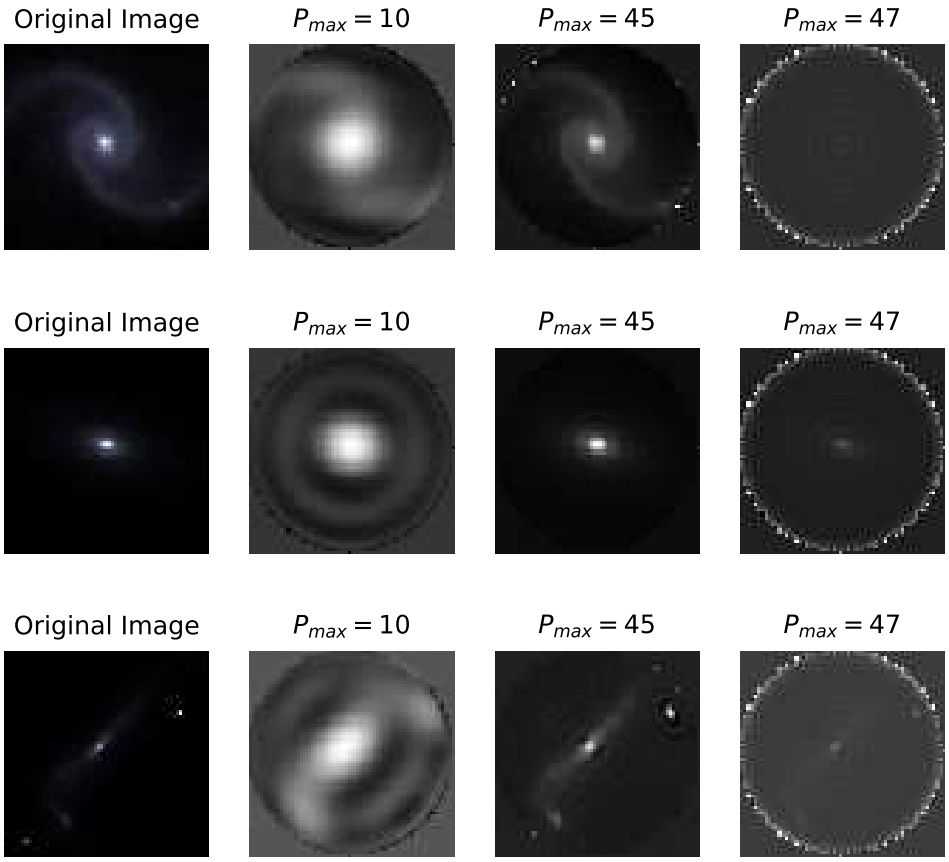


Figure 6: From left to right, panels represent the original and reconstructed images with the different maximum order numbers ($P_{\max}$= 10, 45, and 47), respectively, for a spiral galaxy (top row), elliptical galaxy (middle row), and irregular galaxy (bottom row). Recorded by SDSS survey.

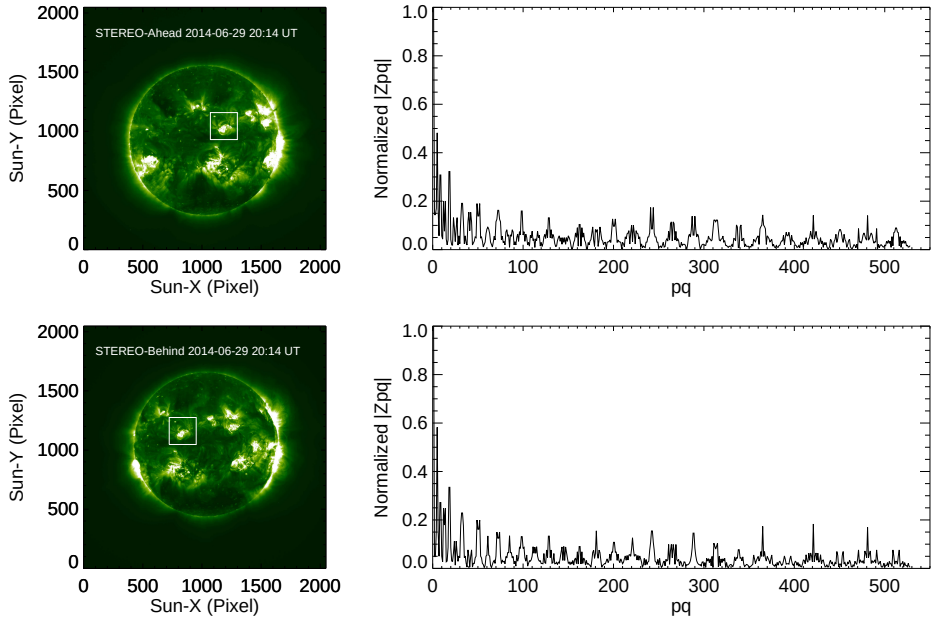


Figure 7: A solar active region indicated by a white box of the EUVI images at 195 Å recorded by STEREO-A (Left top) and STEREO-B (Left bottom). The normalized absolute values of the Zernike moments for $P_{\max}$=31 (Alipour et al., 2019).

Due to the Fourier term in the azimuthal angle function, the absolute value of moments is independent of the objects' rotation angle in the image. Space missions and ground base instruments observe solar features from various perspectives and scales. The Soho was in the first Lagrangian point of the Sun-Earth. STEREO A and B are in Earth's orbit. Figure 7 presents the ZMs of an active region observed by two STEREO A and B. The ZMs are similar from two different viewpoints. The block structures of the ZMs series are identical, with slight differences. These trivial differences may be due to the digital rather than the continuous image. Applying a transformation (to the image centre of brightness) and image normalization, ZMs will be translation and scaling invariances, respectively (see, e.g., Khotanzad and Hong, 1990)
The SoHO/EIT and SDO/AIA resolutions are 0.6 and 2.4, respectively. The ZMs for the active region (Figure 8) with various resolutions are slightly similar. It seems the ZMs are functions of the morphology and geometry of the objects and depend less on the object's size.

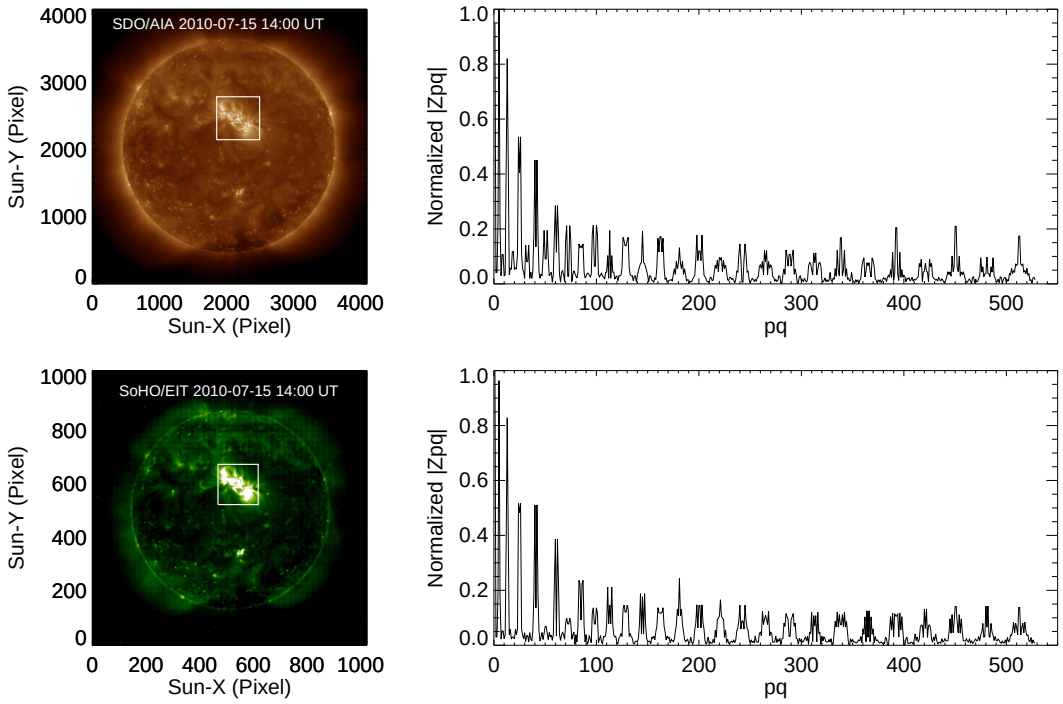


Figure 8: The white boxes represent of an active region observed by SDO/AIA image at 193 Å (Left top panel) and SoHO/EIT (Left bottom panel).(Right) The normalized absolute value of Zernike moments for two SDO and SoHo views (Alipour et al., 2019).

# 5 Python code for ZMs

The Python code is available at Github (`https://github.com/hmddev1/ZEMO`) and PyPI (`https://pypi.org/project/ZEMO/1.0.0/`). The Python code calculates ZMs for a given image. Alipour and Safari (2015) and Alipour et al. (2019) used the primitive code for calculating ZMs of solar features. The code includes the following functions:

- The zernike_order_list function calculates factorials, $p$ (order numbers)-indices, and $q$ (repetition numbers)-indices for a given maximum order number of Zernike polynomials.
- The robust_fact_quot function removes common elements from lists and calculates product quotients.
- The zernike_bf function generates Zernike basis functions stored in a complex-valued grid.
- The zernike_mom function calculates Zernike moments by summing the product of the image and basis functions.
- The zernike_rec function reconstructs an image by summing the weighted Zernike basis functions via ZMs.

The code includes checks for data validity, such as square image size matching, and prints informative error messages.

# 6 Conclusion

The Zernike polynomials indicate the distance along the radius and azimuthal angle. Equation (5) shows the image function weighted by the radial part $rR_{pq}(r)$. We note that $|R_{pq}(r)| < 1$ and $|rR_{pq}(r)| < r$ within a unit circle that shows that the edge's pixels have more extensive weights than the center pixels. The higher-order Zernike polynomials will show more oscillations to extract information on the image details along the radius from the origin to the perimeter (Shutler and Nixon, 2001).
Why are ZMs helpful in expressing an image?

- The Zernike basis is orthogonal and complete set functions, so ZMs are unique quantities features.
- We may reconstruct the original image by a finite number of moments.
- ZMs are slightly sensitive to noises.
- The magnitude of ZMs is rotation invariant. Image normalization makes translation and scale invariants for ZMs.

These reasons showed the capability of ZMs to describe an image to apply machine learning to identify and track the features in several disciplines. We published the Python code via Github and PyPI.

# References


Alipour, N., Mohammadi, F., and Safari, H. (2019). Prediction of Flares within 10 Days before They Occur on the Sun. *Astrophysical Journal, Supplement*, 243(2):20.

Alipour, N. and Safari, H. (2015). Statistical properties of solar coronal bright points. *The Astrophysical Journal*, 807(2):175.

Alipour, N., Safari, H., and Innes, D. E. (2012). An Automatic Detection Method for Extreme-ultraviolet Dimmings Associated with Small-scale Eruption. *Astrophysical Journal*, 746:12.

Alipour, N., Safari, H., Verbeeck, C., Berghmans, D., Auchère, F., Chitta, L. P., Antolin, P., Barczynski, K., Buchlin, É., Aznar Cuadrado, R., Dolla, L., Georgoulis, M. K., Gissot, S., Harra, L., Katsiyannis, A. C., Long, D. M., Mandal, S., Parenti, S., Podladchikova, O., Petrova, E., Soubrié, É., Schühle, U., Schwanitz, C., Teriaca, L., West, M. J., and Zhukov, A. N. (2022). Automatic detection of small-scale EUV brightenings observed by the Solar Orbiter/EUI. *Astronomy and Astrophysics*, 663:A128.

Aschwanden, M. J. (2010). Image processing techniques and feature recognition in solar physics. *Solar Physics*, 262(2):235–275.

Belkasim, S., Ahmadi, M., and Shridhar, M. (1996). Efficient algorithm for fast computation of zernike moments. *Journal of the Franklin Institute*, 333(4):577–581.

Capalbo, V., Petris, M. D., Luca, F. D., Cui, W., Yepes, G., Knebe, A., Rasia, E., Ruppin, F., and Ferragamo, A. (2022). Morphological analysis of SZ and x-ray maps of galaxy clusters with zernike polynomials. *EPJ Web of Conferences*, 257:00008.

Chong, C.-W., Raveendran, P., and Mukundan, R. (2003). A comparative analysis of algorithms for fast computation of zernike moments. *Pattern Recognition*, 36(3):731–742.

Doerr, F. and Florence, A. (2020). A micro-xrt image analysis and machine learning methodology for the characterisation of multi- particulate capsule formulations. *International Journal of Pharmaceutics: X*, 2.

Flusser, J. (2000). On the independence of rotation moment invariants. *Pattern Recognition*, 33(9):1405–1410.

Gonzaga, A. and Ferreira Costa, J. A. (1996). Moment invariants applied to the recognition of objects using neural networks. In Tescher, A. G., editor, *Applications of Digital Image Processing XIX*, volume 2847 of *Society of Photo-Optical Instrumentation Engineers (SPIE) Conference Series*, pages 223–233.

Gonzalez, R. and Faisal, Z. (2019). *Digital Image Processing Second Edition*.

Goshtasby, A. (1985). Template matching in rotated images. *IEEE Transactions on Pattern Analysis and Machine Intelligence*, (3):338–344.

Grubbström, R. W. and Tang, O. (2006). The moments and central moments of a compound distribution. *European Journal of Operational Research*, 170(1):106–119.

Gu, J., Shu, H., Toumoulin, C., and Luo, L. (2002). A novel algorithm for fast computation of zernike moments. *Pattern Recognition*, 35(12):2905–2911. Pattern Recognition in Information Systems.

Heywood, M. and Noakes, P. (1995). Fractional central moment method for movement-invariant object classification. *IEE Proceedings-Vision, Image and Signal Processing*, 142(4):213–219.

Honarbakhsh, L., Alipour, N., and Safari, H. (2016). Magnetic Evolution of Mini-Coronal Mass Ejections. *Solar Physics*, 291(3):941–952.

Honarbakhsh, L. and Morra, G. (2023). Classification of IR Images of Small Eruptions at the Erebus Volcano, Antarctica, With Zernike Moments and Support Vector Machine. *Journal of Geophysical Research (Solid Earth)*, 128(6):e2022JB025728.

Hosseini Rad, S., Alipour, N., and Safari, H. (2021). Energetics of Solar Coronal Bright Points. *Astrophysical Journal*, 906(1):59.

Hu, M.-K. (1962). Visual pattern recognition by moment invariants. *IRE Transactions on Information Theory*, 8(2):179–187.

Javaherian, M., Safari, H., Amiri, A., and Ziaei, S. (2014). Automatic method for identifying photospheric bright points and granules observed by sunrise. *Solar Physics*, 289.

Khotanzad, A. and Hong, Y. H. (1990). Invariant image recognition by zernike moments. *IEEE Transactions on pattern analysis and machine intelligence*, 12(5):489–497.

Mitzias, D. A. and Mertzios, B. G. (2004). A neural multiclassifier system for object recognition in robotic vision applications. *Measurement*, 36(3-4):315–330.

Moradkhani, M., Amiri, A., Javaherian, M., and Safari, H. (2015). A hybrid algorithm for feature subset selection in high-dimensional datasets using fica and iwssr algorithm. *Applied Soft Computing*, 35:123–135.

Mukundan, R., Ong, S., and Lee, P. A. (2001). Image analysis by tchebichef moments. *IEEE Transactions on image Processing*, 10(9):1357–1364.

Mukundan, R. and Ramakrishnan, K. R. (1995). Fast computation of legendre and zernike moments. *Pattern Recognit.*, 28:1433–1442.

Nayak, D. R., Dash, R., and Majhi, B. (2018). An improved pathological brain detection system based on two-dimensional pca and evolutionary extreme learning machine. *J. Med. Syst.*, 42(1):1–15.

Niu, K. and Tian, C. (2022). Zernike polynomials and their applications. *Journal of Optics*, 24(12):123001.

Noori, M., Javaherian, M., Safari, H., and Nadjari, H. (2019). Statistics of photospheric supergranular cells observed by SDO/HMI. *Advances in Space Research*, 64(2):504–513.

Papakostas, G. A., Boutalis, Y. S., Karras, D. A., and Mertzios, B. G. (2007). A new class of zernike moments for computer vision applications. *Information Sciences*, 177(13):2802–2819.

Papakostas, G. A., Boutalis, Y. S., Papaodysseus, C., and Fragoulis, D. K. (2006). Numerical error analysis in zernike moments computation. *Image and Vision Computing*, 24(9):960–969.

Raboonik, A., Safari, H., Dadashi, N., and Alipour, N. (2016). Prediction of M and X Solar flares by Using Machine Learning Algorithm. In *41st COSPAR Scientific Assembly*, volume 41, pages D2.5–21–16.

Sadeghi, M., Javaherian, M., and Miraghaei, H. (2021). Morphological-based classifications of radio galaxies using supervised machine-learning methods associated with image moments. *The Astronomical Journal*, 161(2):94.

Shokri, Z., Alipour, N., Safari, H., Kayshap, P., Podladchikova, O., Nigro, G., and Tripathi, D. (2022). Synchronization of small-scale magnetic features, blinkers, and coronal bright points. *The Astrophysical Journal*, 926:42.

Shutler, J. D. and Nixon, M. S. (2001). Zernike velocity moments for description and recognition of moving shapes. In *Proceedings of the British Machine Vision Conference*, pages 72.1–72.10. BMVA Press. doi:10.5244/C.15.72.

Sim, D.-G., Kim, H.-K., and Park, R.-H. (2004). Invariant texture retrieval using modified zernike moments. *Image and Vision Computing*, 22(4):331–342.

Teh, C.-H. and Chin, R. T. (1988). On image analysis by the methods of moments. In *Computer Vision and Pattern Recognition, 1988. Proceedings CVPR'88., Computer Society Conference on*, pages 556–561. IEEE.

Wheatland, M., Alipour, N., Raboonik, A., and Safari, H. (2017). Prediction of solar flares using unique signatures of magnetic field images.

Wolf, C., Taylor, G., Jolion, J.-M., Verne, B. J., and Einstein, A. A. (2011). Learning individual human activities from short binary shape sequences. Technical report, Technical Report LIRIS. Available at http://liris. cnrs. fr/Documents/Liris-5294. pdf.

Yousefzadeh, M., Safari, H., Attie, R., and Alipour, N. (2016). Motion and magnetic flux changes of coronal bright points relative to supergranular cell boundaries. *Solar Physics*, 291.

Zhang, Y., Wang, S., Sun, P., and Phillips, P. (2015). Pathological brain detection based on wavelet entropy and hu moment invariants. *Bio-medical materials and engineering*, 26 Suppl 1:S1283–90.

Zheng, C., Pulido, J., Thorman, P., and Hamann, B. (2015). An improved method for object detection in astronomical images. *Monthly Notices of the Royal Astronomical Society*, 451(4):4445–4459.

Zhenjiang, M. (2000). Zernike moment-based image shape analysis and its application. *Pattern Recognition Letters*, 21(2):169–177.